Available online at www.sciencedirect.com

ScienceDirect

Procedia CIRP 118 (2023) 654–658

www.elsevier.com/locate/procedia

16th CIRP Conference on Intelligent Computation in Manufacturing Engineering, CIRP ICME '22, Italy

Spatio-temporal Analysis of Thermal Profiles in Extrusion-based Additive Manufacturing

Bianca Maria Colosimo, Fabio Caltanissetta*, Emanuele Carraro,

Department of Mechanical Engineering, Politecnico di Milano, Via Giuseppe La Masa 1, 20133, Milan (Italy)

* Corresponding author. Tel.: 39 3245496452; *E-mail address:* fabio.caltanissetta@polimi.it

Abstract

Extrusion-based Additive Manufacturing (AM) processes have recently gained increasing attention in the scientific and industrial communities because of the wide range of processible materials (from thermoplastics to composite and biomaterials), printable volumes, and industrial applications. As for many other AM processes, the actual problems with process stability and repeatability are still limiting the industrial process adoption, as these problems can significantly impact on the final part quality. In this framework, a latest research trend aims at developing in-situ monitoring solutions for inline defect detection, in a zero-waste production perspective. Among the existing in-situ sensing techniques, many studies showed that in-situ thermography represents a viable solution to describe the temperature dynamic and validate the thermal models but very few approaches have been proposed to quantitively study the temperature evolution to quickly detect process instabilities.
This paper presents a new approach to quickly analyse the temporal dynamic of temperature in the printed layer while providing a spatial mapping of the temperature homogeneities. Compared with previous methods, the current one has the main novelty feature of combining both the spatial and temporal signature in a synthetic mapping that allows to detect unstable or unusual problems. In order to show the effectiveness of the proposed solution, a real case study of Big Area Additive Manufacturing (BAAM) for composite materials is considered. The study shows that the provided method can clearly enhance defect detection and represents a new solution for detecting anomalous areas where thermal profiles behave differently with respect to the surrounding areas. The same methodology underlined the thermal evolution complexity in the BAAM case study and enabled the detection of local flaws, i.e., hot and cold spots.

Keywords: Additive manufacturing; BAAM; In-situ monitoring; Thermography; Spatio-temporal indicators; Moran index

1. Introduction

In the past years, Additive Manufacturing (AM) technologies have drastically changed the manufacturing panorama, introducing a vast range of new possibilities in terms of product design, materials, and applications. Extrusion-based AM processes are currently under the spotlight because of the extensive range of printable materials (techno-polymers, ceramics, composite, metals etc.) and the large variability of printable sizes, ranging from millimeters to meters. Despite of this significant advantages, the low repeatability and stability have limited the diffusion of extrusion-based AM in industrial world, being unable to achieve quality standards required for final products.

To tackle this issue, the scientific and the industrial community have recently proposed methods based on in-situ monitoring to prevent the arising of defects, in a first-time-right production perspective [1,2]. Among many available information sources, the temperature evolution has found significant interest, since it allows the identification of different

10.1016/j.procir.2023.06.112

anomalies linked to final part quality, such as lack of bonding within layers and geometry inaccuracy [3,4]. So far, the existing studies on temperature analysis focused on the description of in-situ sensing setups (mainly based on infrared cameras) [5-7], the validation of simulated thermal models [8-10], and the qualitative interpretation of temperature evolution [11,12].

Nevertheless, there is a lack of effort devoted to the use of artificial intelligence and statistical data mining aimed to automatically detect the presence of process instabilities [2]. These tasks are far from being trivial, considering different sources of complexity. First, the high dimensionality of input data, which, in case of thermal profiles extracted from IR videos, are related to the camera resolution and frame rate acquisition. Then, the search of reliable analytical or numerical thermal models is still in progress, thus the comparison of in-situ thermal acquisition with a ground truth is still not possible. Finally, the infrared data are characterized by a double nature, which is jointly related to time and space. Indeed, temperature values depends on the time after material extrusion and their location within the layer.

To tackle all these issues, this paper proposes the adoption of simple, computationally efficient, and model-free indicators for spatio-temporal analysis. Indicators have been proposed in the literature to study the spatial [13] and the temporal dimensions [14,15] separately.

In this paper, a methodology for spatio-temporal thermal data analysis of AM processes is proposed. The methodology is inspired by the paper by Gao et al. [8] in the context of data analysis, where a new version of the Moran's index [13] indicator is proposed to include a descriptor of temporal correlation, namely the *z* index [4]. The effectiveness of this newly defined index is firstly explored in a simulation scenario, where different clusters of anomalous thermal profiles are included in the in-control profiles. These preliminary tests show the effectiveness of the proposed solution in describing and highlighting spatio-temporal events. These findings are then explored in the real case study, where the spatio-temporal indicators allow one to explore the complexity of the temperature dynamics (despite the toolpath simplicity) and are useful for visual inspection of local thermal flaws as hot and cold spots, i.e., spatially clustered temperature profiles which differ from the average thermal behavior.

2. Methodology

Assume a dynamic process has both a spatial and temporal signature that need to be investigated [16]. Let $\boldsymbol{x_{i,t}}$ represent the value of the time series in the location *i* at time *t,* a first ingredient of a spatio-temporal indicator is the *CORT* component, which is given by the cross correlation between the thermal profile $\boldsymbol{x_i}$ observed at location *i* and the average profile $\bar{\boldsymbol{x}}$ observed over all the spatial locations in the time interval [1, T]:

$$CORT(\boldsymbol{x}_i, \bar{\boldsymbol{x}}) = \frac{\sum_t^{T-1}(x_{i,t+1} - x_{i,t})(\bar{x}_{t+1} - \bar{x}_t)}{\sqrt{\sum_t^{T-1}(x_{i,t+1} - x_{i,t})^2}\ \sqrt{\sum_t^{T-1}(\bar{x}_{t+1} - \bar{x}_t)^2}} \quad (1)$$

The *CORT* indicator assumes values in the interval [-1,1], where values close to 1 (or -1) represent conditions of positive (or negative) correlation, i.e., situations where $\boldsymbol{x_i}$ and $\bar{\boldsymbol{x}}$ increase or decrease simultaneously in the same (or opposite) directions. On the other side, values of *CORT* close to 0 represent the lack of significant correlation between the two-time series. Usually, the CORT index is transformed by applying the function $\boldsymbol{\varphi}$:

$$\varphi(CORT\ (\boldsymbol{x}_i, \bar{\boldsymbol{x}})) = \frac{2}{1 + e^{2*CORT(\boldsymbol{x}_i, \bar{\boldsymbol{x}})}} \quad (2)$$

which is an exponential adaptive tuning function used to remap the CORT index in a new range (0, 2) such that the strongest is the correlation of the *i*-th profile with the average profile, the largest is the $\varphi\big(\ CORT(\boldsymbol{x}_i, \bar{\boldsymbol{x}})\big)$ component.

In order to augment the patter similarity with a second element to describe the magnitude/level effect, a new index is defined which includes information on the area underlying the thermal profile. Let v_i and $\bar{v}$ represent the areas under the curve $\boldsymbol{x}_i$ and $\bar{\boldsymbol{x}}$, respectively:

$$v_i = \int_1^T \boldsymbol{x}_i\, dt;\ \ \bar{v} = \int_1^T \bar{\boldsymbol{x}}\, dt. \quad (3)$$

The new $\boldsymbol{z_i}$ indicator is eventually computed to combine the patter similarity described in $\boldsymbol{\varphi\big(\ CORT(x_i, \bar{x})\big)}$ with the size/level effect computed as the difference between the area underneath the *i*-th profile and one underneath the average thermal profile:

$$z_i = \varphi(\ CORT(\boldsymbol{x}_i, \bar{\boldsymbol{x}})) \cdot (v_i - \bar{v}\ ) \quad (4)$$

As that $\boldsymbol{\varphi\big(CORT(x_i, \bar{x})\big)}$ is always above 0, the sign of $\boldsymbol{z_i}$ is determined by the area component. Profiles whose underlying area is larger (smaller) than the area under the average profile will get a positive (negative) value of $\boldsymbol{z_i}$.

The description of the temporal dynamic provided by the z_i index is eventually combined with the spatial information describing the association of thermal profiles in the neighborhoods of the i-th location:

$$I_i = \frac{(z_i - \bar{z})}{\sum_i\ (z_i - \bar{z})^2} \cdot \sum_j w_{ij}(z_j - \bar{z}) \quad (1)$$

here $\boldsymbol{w_{ij}}$ is a weight expressing the spatial proximity between locations *i* and *j≠i.* given by the inverse of the Euclidian distance and $\bar{\boldsymbol{z}}$ is the average value of $\boldsymbol{z_i}$ in all the locations.

The newly defined local Moran's index I_i expresses the spatial correlation between the element z_i observed in the neighbors. If the location *i* is surrounded by elements with similar (dissimilar) values, then $I_i > 0$ ($I_i < 0$). If it is surrounded by both similar and dissimilar values in a random arrangement, then $I_i \approx 0$.

In the context of Extrusion-based AM, the spatio-temporal indicator is applied to temperature profiles, extracted at predefined locations in each layer. The thermal

cooling pattern at each location can be studied through the *z* Local Moran's *I* indexes.

3. Simulation Study

In this section, the behavior of the spatio-temporal indicators is tested using simulation. IR thermal data are simulated by generating 81 temperature profiles, each associated to a location in a 9X9 grid. Each profile $\boldsymbol{x_i}$ is drawn considering a second-order linear model, similar to temperatures profiles observed in real case studies dealing with Extrusion-based AM [11]:

$$x_{i,t} = e^{(\beta_{0i}+\beta_{1i}t+\beta_{2i}t^2+\varepsilon)} \quad (2)$$

where $\boldsymbol{x_{i,t}}$ is a function of time *t* and $\boldsymbol{\beta_{0i}, \beta_{1i}}$ **and** $\boldsymbol{\beta_{2i}}$ are the coefficients of a second order polynomial function, while $\boldsymbol{\varepsilon}$ ~iid $N(0,\boldsymbol{\sigma^2})$. A clustered anomalous area is simulated considering a 3x3 cells where the $\boldsymbol{\beta_1}$'s coefficients are altered. More in details, an out-of-control thermal profiles is assumed considering altered values of $\boldsymbol{\beta_{1i}}^*$ with respect to the in-control state $\boldsymbol{\beta_{1i}}$, i.e., $\boldsymbol{\beta_{1i}}^* = \boldsymbol{K\beta_{1i}}$, where K was initially set equal to 3. Hereafter, a visualization of the simulated temperature profiles and their spatial location is provided (**Error! Reference source not found.**).

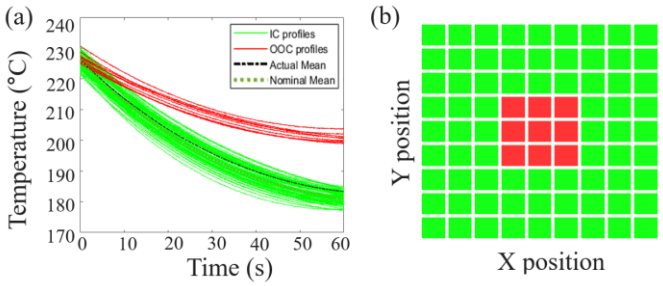

Fig. 1. (a) Simulated Temperature profiles. Green lines represent the in-control - IC - temperature profiles, while the red lines are the altered profiles - OOC. (b) Spatial disposition of IC e OOC temperature profiles.

Error! Reference source not found. depicts the results of the computation of *z* and local Moran's indexes. The *z* indicator highlights all the defective cells, taking high and positive values for the out-of-control profiles. The positive sign is determined by the difference between the areas under the curve, as specified in formula (3), since the alteration of curve slope is positive. From the visual inspection of Error! Reference source not found., we can see that the Moran index *I* emphasizes the out-of-control cluster, underlying the presence of similar and spatially adjacent temperature profiles which deviate from the average temperature pattern. When no anomalies are present, the Moran's index smooths the *z* values, thus increasing the contrast between defective and non-defective areas.

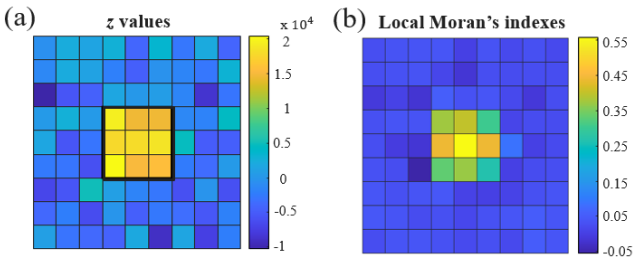

Fig. 2. (a) *z* indexes and (b) local Moran's indexes visualization through heatmap; the defective region is highlighted with thick borders.

The effectiveness of the spatio-temporal indicators is further tested in terms of robustness towards defect size (D) and defect magnitude (K), i.e., by changing the number of defective profiles in each matrix and the deviation of β_{1i} (see **Error! Reference source not found.**).

Results show that, for defects of small to medium sizes, the local Moran's index correctly highlights the defective areas, regardless the defect intensity. When the defective area is extended and takes more than a half of the total number of profiles, the distinction between in-control and out of control areas is less clear, particularly in proximity of the defective area's borders.

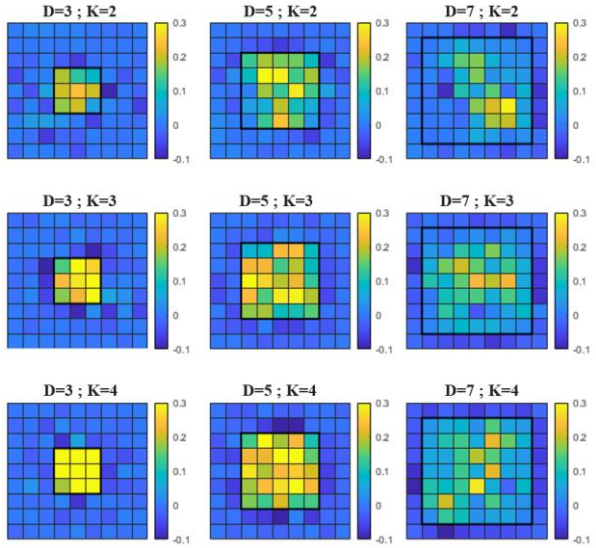

Fig. 3. Local Moran's indexes for different values of defect dimension (D) and magnitude (K).

4. Case Study

The dataset exploited for the real case study consists of the temperature profiles extracted from an infrared video of a Big Area Additive Manufacturing (BAAM) process [19]. The part under investigation was manufactured by the large-scale printer developed at the Oak Ridge National laboratories in collaboration with Cincinnati Incorporated [20]. Acrylonitrile Butadiene Styrene (ABS) with 20% of chopped carbon fibers weight is used to print a connected serpentine pattern, made by five long connected beads. This toolpath is repeated for 15 layers.

Extruder temperature was set at 230°C, while the building platform was pre-heated at 90°C. Extruder speed was 63.5

mm/s, so that a single layer printing lasts around 70 seconds. The infrared video was acquired at a framerate of 30 fps using a FLIR A35 thermal camera (FLIR® Systems Inc, Wilsonville, U.S.), positioned near the build area (approximately 1.3 m from the target object) with an inclination with respect to the building platform of around 45°.

For each layer, temperature profiles are extracted from 506 Regions of Interest (ROI), placed along the extruder's toolpath (see **Error! Reference source not found.**). An ID value was assigned to each ROI, starting from the initial position of the extruder (ROI ID=1), following the extruder toolpath up to the end of layer extrusion (ROI ID=506).

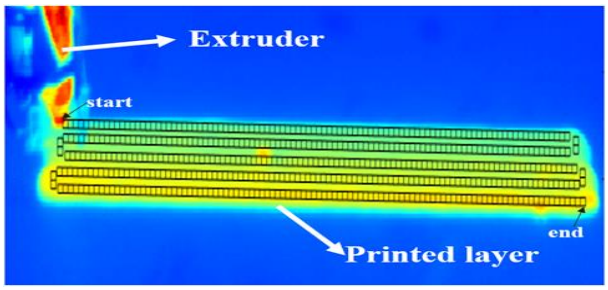

Fig. 4. Example of a frame taken from the analysed IR video. Black squares highlight the ROI under investigation.

4.1. Analysis of thermal evolution

Figure 5 depicts the average z values and local Moran's index across the layers.

Despite the simplicity of the chosen extruder toolpath, both the indexes show a quite complex behavior, highlighting the presence of relevant patterns.

The z index takes values lower than 0 in the first and last beads. Thus, in these areas the measured thermal profiles $\boldsymbol{x_i}$ stand below the layer's average profile $\bar{\boldsymbol{x}}$. The first bead shows also a sudden temperature jump right after the layers' starting points, which progressively decreases towards the end of the bead. The temperature instability in the first bead can be explained with a machine transient state at the beginning of each layer, probably caused by the acceleration and deceleration of the extruder's head, as well as change in the extrusion feed rate. Areas with low values of z are also present at the beginning and at the end of each bead, i.e., where the extruder changes direction before printing a new bead. In general, the ROIs placed on the external borders display a faster cooling with respect to the average behavior, due to the lower heat retention. Indeed, they have less surface in contact with the rest of the printed layer with respect to the central beads. Similar results have been observed in [8].

Concerning the rest of the printed beads, the central part of the layers shows positive and higher values of z indexes, indicating a large area where thermal profiles stand above the average one.

The bottom panel of Figure 5 depicts the average evolution of the local Moran's index across. It highlights different zones with high spatial autocorrelation, i.e., clustered areas where thermal profiles behave in the same manner. Two areas with high local Moran's index are present at the beginning and at the end of the printed layer. As discussed before, in these clusters z takes low values, far from those of the surrounding ROIs. Other similar clusters are visible in the beads turning point, particularly on the left size. Again, in these points z values are lower than 0. Finally, an extended area of positive spatial correlation can be observed in the layers' left size, particularly between the first and the third bead, where z values above 0 always occur, signaling an area that is hotter than the rest of the layer.

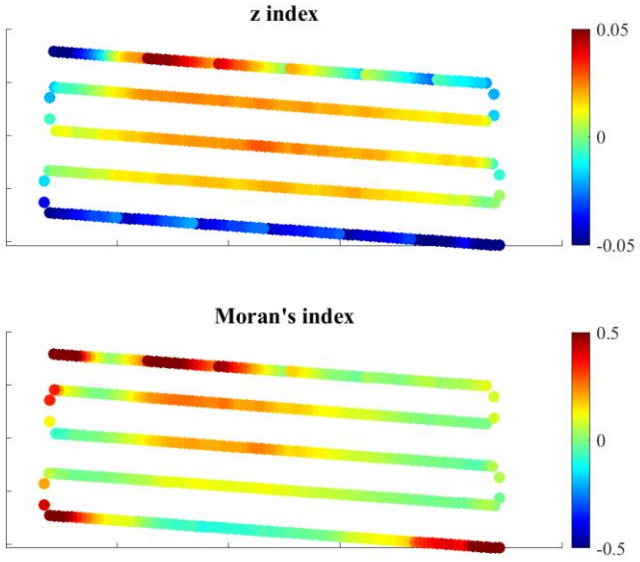

Fig. 5. Top: spatial representation of z values and (b). local Moran's indexes. Each point represents the index mean value across the 15 layers.

5. Conclusions

This paper proposed a new methodology that can be used as a powerful tool to gain a deep understanding of the thermal behavior in extrusion-based AM processes. The main advantage of the proposed solution relies on its capability to jointly capture the temporal and the spatial information underlying the observed phenomenon. The effectiveness of the proposed solution was explored considering both a simulation and a real case study, where the temperature dynamics observed in thermal videos acquired in Big Area Additive Manufacturing was of interest. The two proposed indicators were indeed able to underline the presence of different areas characterizes by peculiar thermal behaviors, compared with the average temperature profile. Moreover, local Moran's indexes were useful to identify areas with high spatial correlation.

Future developments encompass the expansion of simulation to different scenarios, the combination of the current methodology with the *a priori* knowledge on the average (or target) thermal profile and the inclusion of the proposed solution as a basic element of a new procedure for statistical process monitoring or control to take full advantage of the proposed methodology for in-situ in-line AM process monitoring.

6. Acknowledgements

The present research was partially supported by "PROGETTO ROBERTO ROCCA". The authors are grateful to Prof. John Hart (Massachusetts Institute of Technology) and the Oak Ridge National Laboratory (ORNL), for their contribution to the experimental data.

References

[1] Fu, Y., Downey, A., Yuan, L., Pratt, A., & Balogun, Y. (2021). In situ monitoring for fused filament fabrication process: A review. Additive Manufacturing, 38, 101749.

[2] Oleff, A., Küster, B., Stonis, M., & Overmeyer, L. (2021). Process monitoring for material extrusion additive manufacturing: a state-of-the-art review. Progress in Additive Manufacturing, 1-26.

[3] Attoye, S. O. (2018). A study of fused deposition modeling (FDM) 3-D printing using mechanical testing and thermography (Doctoral dissertation).

[4] Zhang, J., Wang, X. Z., Yu, W. W., & Deng, Y. H. (2017). Numerical investigation of the influence of process conditions on the temperature variation in fused deposition modeling. Materials & Design, 130, 59-68

[5] Dinwiddie, R. B., Kunc, V., Lindal, J. M., Post, B., Smith, R. J., Love, L., & Duty, C. E. (2014, June). Infrared imaging of the polymer 3D-printing process. In Thermosense: Thermal Infrared Applications XXXVI (Vol. 9105, p. 910502). SPIE.

[6] Malekipour, E., Attoye, S., & El-Mounayri, H. (2018). Investigation of layer based thermal behavior in fused deposition modeling process by infrared thermography. Procedia Manufacturing, 26, 1014-1022.

[7] Seppala, J. E., & Migler, K. D. (2016). Infrared thermography of welding zones produced by polymer extrusion additive manufacturing. Additive manufacturing, 12, 71-76.

[8] Choo, K., Friedrich, B., Daugherty, T., Schmidt, A., Patterson, C., Abraham, M. A., ... & MacDonald, E. (2019). Heat retention modeling of large area additive manufacturing. Additive Manufacturing, 28, 325-332.

[9] Compton, B. G., Post, B. K., Duty, C. E., Love, L., & Kunc, V. (2017). Thermal analysis of additive manufacturing of large-scale thermoplastic polymer composites. Additive Manufacturing, 17, 77-86.

[10] Costa, S. F., Duarte, F. M., & Covas, J. A. (2017). Estimation of filament temperature and adhesion development in fused deposition techniques. Journal of Materials Processing Technology, 245, 167-179.

[11] Ferraris, E., Zhang, J., & Van Hooreweder, B. (2019). Thermography based in-process monitoring of Fused Filament Fabrication of polymeric parts. CIRP Annals, 68(1), 213-216.

[12] Malekipour, E., Attoye, S., & El-Mounayri, H. (2018). Investigation of layer based thermal behavior in fused deposition modeling process by infrared thermography. Procedia Manufacturing, 26, 1014-1022.

[13] Anselin, L. (1995). Local indicators of spatial association—LISA. Geographical analysis, 27(2), 93-115.

[14] Lhermitte, S., Verbesselt, J., Verstraeten, W. W., & Coppin, P. (2011). A comparison of time series similarity measures for classification and change detection of ecosystem dynamics. Remote sensing of environment, 115(12), 3129-3152.

[15] Chouakria, A. D., & Nagabhushan, P. N. (2007). Adaptive dissimilarity index for measuring time series proximity. Advances in Data Analysis and Classification, 1(1), 5-21

[16] Gao, Y., Cheng, J., Meng, H., & Liu, Y. (2019). Measuring spatio-temporal autocorrelation in time series data of collective human mobility. Geo-spatial Information Science, 22(3), 166-173.

[17] Dubé, J., & Legros, D. (2013). A spatio‐temporal measure of spatial dependence: An example using real estate data. Papers in Regional Science, 92(1), 19-30.

[18] Lee, J., & Li, S. (2017). Extending moran's index for measuring spatiotemporal clustering of geographic events. Geographical Analysis, 49(1), 36-57.

[19] F. Caltanissetta, G. Dreyfus, A. J. Hart and B. M. Colosimo, "In-situ monitoring of Extrusion-based processes via thermal videoimaging with application to Big Area Additive Manufacturing (BAAM)," submitted paper.

[20] Love, L. J., & Duty, C. (2015). Cincinnati big area additive manufacturing (BAAM). Oak Ridge, TN.